Octreotide attenuates intestinal barrier damage by maintaining basal autophagy in Caco2 cells

XIAOLI LIU[1*], YAN ZHOU[2*], YU ZHANG[3*], XIGANG CUI[4], DONGLIN YANG[1] and YULING LI[1]

[1]School of Basic Medical Sciences, Binzhou Medical University; [2]Department of Gastrointestinal Surgery, Yantai Mountain Hospital; [3]Department of Gastrointestinal Surgery, Yantai Affiliated Hospital of Binzhou Medical University, Yantai, Shandong 264003; [4]Department of Gastrointestinal and Thyroid Surgery, The Affiliated Yantai Yuhuangding Hospital of Qingdao University, Yantai, Shandong 264000, P.R. China

Received September 20, 2023; Accepted March 12, 2024

DOI: 10.3892/mmr.2024.13214

Abstract. The intestinal mucosal barrier is of great importance for maintaining the stability of the internal environment, which is closely related to the occurrence and development of intestinal inflammation. Octreotide (OCT) has potential applicable clinical value for treating intestinal injury according to previous studies, but the underlying molecular mechanisms have remained elusive. This article is based on a cell model of inflammation induced by lipopolysaccharide (LPS), aiming to explore the effects of OCT in protecting intestinal mucosal barrier function. A Cell Counting Kit-8 assay was used to determine cell viability and evaluate the effectiveness of OCT. Gene silencing technology was used to reveal the mediated effect of somatostatin receptor 2 (SSTR2). The changes in intestinal permeability were detected through trans-epithelial electrical resistance and fluorescein isothiocyanate-dextran 4 experiments, and the alterations in tight junction proteins were detected using immunoblotting and reverse transcription fluorescence-quantitative PCR technology. Autophagosomes were observed by electron microscopy and the dynamic changes of the autophagy process were characterized by light chain (LC)3-II/LC3-I conversion and autophagic flow. The results indicated that SSTR2-dependent OCT can prevent the decrease in cell activity. After LPS treatment, the permeability of monolayer cells decreased and intercellular tight junctions were disrupted, resulting in a decrease in tight junction protein zona occludens 1 in cells. The level of autophagy-related protein LC3 was altered to varying degrees at different times. These abnormal changes gradually returned to normal levels after the combined application of LPS and SSTR2-dependent OCT, confirming the role of OCT in protecting intestinal barrier function. These experimental results suggest that OCT maintains basal autophagy and cell activity mediated by SSTR2 in intestinal epithelial cells, thereby preventing the intestinal barrier dysfunction in inflammation injury.

Correspondence to: Dr Yuling Li, School of Basic Medical Sciences, Binzhou Medical University, 346 Guanhai Road, Yantai, Shandong 264003, P.R. China
E-mail: lee845@126.com

*Contributed equally

Key words: octreotide, somatostatin receptors, autophagy, intestinal epithelial cells, intestinal barrier function, Caco2 cells

Introduction

The intestinal epithelial barrier is one of the most important immune barriers of defense against invasive symbiotic bacteria and intestinal pathogens (1). Damage to the intestinal epithelial barrier may lead to the translocation of bacteria and metabolites into the bloodstream and tissues (2,3). In severe cases, this translocation may trigger systemic inflammation and multiple organ dysfunction syndrome (4). Numerous pathological states, such as ischemia reperfusion injury, inflammation and cancers, such as liver or pancreatic cancer (5), cause damage to the intestinal mucosal barrier (6), leading to complexities in clinical practice and poor patient prognosis (7). Therefore, current research is focused on exploring novel methods for protecting and repairing intestinal barrier function.

Octreotide (OCT) is a synthetic octapeptide derivative of natural somatostatin (8). Results of previous studies demonstrated that OCT may prevent diarrhea caused by chemotherapy, intestinal injury caused by severe pancreatitis and inflammatory bowel disease (IBD) (9-11). Thus, OCT may exhibit potential in the treatment of intestinal injury.

Somatostatin receptors (SSTRs) are G-protein-coupled receptors that are widely expressed on cell membranes in the human brain and kidney (12,13), and in colon tissue (14). Numerous previous studies on SSTRs have focused on their use in preventing tumor cell proliferation (15-17). Somatostatin binds to SSTRs to exert effects on cells (12,18). Results of previous studies revealed that out of the five subtypes of SSTRs, subtypes 2, 3 and 5 exhibit a high affinity for OCT (8,19). Although somatostatin protects the intestinal mucosal barrier by regulating the expression of tight junction (TJ) proteins (8,20-23), the specific molecular mechanisms remain to be fully elucidated.

Autophagy is a process in which cytoplasmic proteins or organelles are phagocytosed into vesicles that fuse with

lysosomes. Following the formation of autophagy lysosomes, all contents of the lysosome are degraded (24-26). Physiologically, autophagy is required for cell metabolism and the renewal of intracellular organelles. Results of previous studies demonstrated that autophagy in intestinal epithelial cells is directly associated with TJ and intestinal epithelial barrier function (27,28).

Lipopolysaccharide (LPS) is unique to the outer membrane of Gram-negative bacteria and is involved in intestinal epithelial innate immunity (29). LPS triggers an inflammatory signaling cascade to induce TJ dysfunction, resulting in intestinal epithelial barrier dysfunction (30,31). Therefore, the present study aimed to explore the effects of OCT on autophagy and SSTR function using LPS-induced Caco2 cells. In addition, the effects of OCT on TJ and intestinal mucosal barrier function were investigated by western blot and reverse transcription-quantitative (RT-q)PCR. The present study provides novel insight into potential methods for the protection and repair of the intestinal epithelial barrier. Furthermore, results of the present study may provide a novel theoretical basis for the treatment of intestinal mucositis in clinical practice.

Materials and methods

Cell culture and treatment. The human colon adenocarcinoma cell lines Caco2 and Sw480 were obtained from Professor Zunling Li and the identity of the cell lines was confirmed by short tandem repeat sequencing. Cells were initially purchased from the American Type Culture Collection. Caco2 cells were cultured in minimum essential medium (including non-essential amino acid; cat. no. PM150410; Sigma-Aldrich; Merck KGaA) containing 20% fetal bovine serum (Thermo Fisher Scientific, Inc.) and stored at 37˚C under 5% CO_2 with saturated humidity. Sw480 cells were cultured in DMEM (cat. no. RNBL7920; Sigma-Aldrich; Merck KGaA) containing 10% fetal bovine serum and stored under the same conditions. They were passaged once every other day and cells in the logarithmic growth phase were used for experimental research.

OCT and LPS treatment in vitro. The treatment method for LPS (cat. no. L4391; Sigma-Aldrich; Merck KGaA) for the two cell lines was performed by adding it to the corresponding culture medium with a final concentration of 100, 50, 10, 1 and 0.1 μg/ml for different durations. OCT (cat. no. HY-17365; MedChemExpress) with a final concentration of 10, 20 or 50 μM was added to the corresponding culture medium 2 h before the addition of LPS. Caco2 cells were inoculated into a 96-well plate with an initial density of $5x10^4$ cells/well and Sw480 were inoculated with an initial density of $6x10^4$ cells/well. In subsequent experiments, the cells were divided into three groups: Control, 50 μg/ml LPS and 10 μM OCT. The control group was left untreated. For the LPS + OCT group, cells were first pretreated with OCT for 2 h and then coincubated with LPS for 24 h, and then various indicators were detected.

Interference with SSTR2 using small interfering (si)RNA. Cells were inoculated into a six-well plate at a density of $5x10^5$ cells/per well and they were allowed to adhere to the bottom of the wells and grow to 50-70% confluence. The instructions provided by the manufacturer of GP-transfect mate (Suzhou Jima Gene, Co., Ltd.) were followed to transfect the cells and the medium was changed 4-6 h after transfection. The total RNA or protein were extracted for detection at 48-72 h after transfection. The siRNA sequences were synthesized by Jima Gene Co., Ltd. The siRNA sets were as follows: Negative Control, 5'-UUCUCCGAACGUGUCACG UTT-3' (sense) and 5'-ACGUGACACGUUCGGAGAATT-3' (anti-sense); SSTR2-Homo-1097 5'-GCUCCUCUAAGAGGA AGAATT-3' (sense) and 5'-UUCUUCCUCUUAGAGGAG CTT-3' (anti-sense); SSTR2-Homo-1264 5'-GUCCUCACC UAUGCUAACAAT-3' (sense) and 5'-UGUUAGCAUAGG UGAGGACTT-3' (anti-sense); SSTR2-Homo-1049 5'-GCU ACCUGUUCAUUAUCAUTT-3' (sense) and 5'-AUGAUA AUGAACAGGUAGCTT-3' (anti-sense).

Cell viability assay. A CCK-8 kit (cat. no. C0038; Beyotime Institute of Biotechnology) was used to detect the viability of the cells treated with the drug. Cells with a density of $5x10^4$ cells/well were seeded into a 96-well plate and cultured for 24 h until they exhibited adherent growth according to the instructions in the manual, and the cells were then stimulated with drugs for 24 h at 37˚C. Subsequently, the cells were incubated with CCK-8 solution for 1 h at 37˚C and the absorbance at 450 nm was detected with a microplate reader. Each experimental condition in each group was set up in three wells. Although the control group had three repeated experiments, it has been normalized as a reference standard for activity calculation.

Western blot analysis. First, cells were cultured in six-well plates at a density of $1x10^6$ cells/well. After 24 h of cell adhesion and growth, LPS and OCT were added to pretreat the cells. The whole-cell protein was extracted according to the instructions provided by the RIPA manufacturer, and the cell pellet was resuspended using a RIPA mixture (cat. no. R0020; Beyotime Institute of Biotechnology) containing PMSF (cat. no. P0100) and phosphatase inhibitor (cat. no. P1082; Beyotime Institute of Biotechnology), followed by 30 min of incubation in an ice bath, during which repeated pipetting was performed every 5 min to ensure full cells lysis. Following centrifugation at 12,000 x g for 20 min, the extracted protein was obtained as the supernatant. The protein concentration was then measured by using a Nanodrop 2000c (Thermo Fisher Scientific, Inc.). Protein samples (10-20 μg) were then separated on 10 or 12% gels using SDS-PAGE. The protein in the gel was then transferred to a nitrocellulose membrane and the nonspecific binding sites on the membrane were blocked for 2 h at room temperature with 5% non-fat milk. The membranes were incubated with primary antibody overnight at 4˚C, and subsequently, they were incubated with horseradish peroxidase-labeled secondary antibody for 1 h at room temperature. Finally, the enhanced luminescent agent A solution and stabilizer B solution (cat. no. BL520B1/BL520B2; Biosharp) were mixed in a 1:1 ratio to visualize the protein bands. The primary antibodies included the following: Antibodies against microtubule-associated protein 1 light chain 3B (LC3; cat. no. ab192890; 1:1,500 dilution; Abcam), zona occludens 1 (zo-1; cat. no. 10019107; 1:1,500 dilution; Proteintech Group, Inc.), GAPDH (cat. no. AF7021; 1:8,000

dilution; Affinity Biosciences), SSTR2 (cat. no. YT-5740), SSTR3 (cat. no. YN-2540), SSTR5 (cat. no. YN-2541; all 1:1,000 dilution; ImmunoWay Biotechnology), goat-anti mouse (cat. no. orb229658; 1:8,000 dilution; Biorbyt) and goat anti-rabbit (cat. no. ZB-2301; 1:8,000 dilution; Zhongshan Jinqiao Biotechnology Co., Ltd.). The intensity of the bands was quantified using ImageJ software version 1.49 (National Institutes of Health).

LC3 double label adenovirus transfection. The target cells were inoculated onto a 24-well plate at a concentration of $1x10^5$ cells/well, and it was ensured that the cell convergence rate is between 50 and 70% when cells were transfected with the Ad-monomeric red fluorescence protein (mRFP)-green fluorescence protein (GFP)-LC3 adenovirus (Hanheng Biotechnology Co., Ltd.) the next day. According to the instructions and technical guidance, the virus was added to the culture medium, left to incubate for 3 h at 37˚C, and the medium was then replaced with fresh culture medium. After 24 h, GFP and RFP expression may be observed, and cell fixation, sealing (mounting medium antifading; Beijing Solarbio Technology Co., Ltd.) and imaging analysis may be performed from 36 to 48 h. Laser confocal microscopy imaging (Leica Microsystems GmbH) was used to capture and manually count autophagic dots. Images were captured using a x40 objective and the experiment was repeated three times; during each repetition, three views were selected to count the fluorescent dots.

Immunofluorescence. Cells were diluted to a density of $5x10^4$ after cell counting and seeded on cover glasses in a 24-well plate in advance. After transfecting cells in a 24-well plate with Ad-mRFP-GFP-LC3 adenovirus for 48 h, they were fixed with 4% paraformaldehyde for 15 min at room temperature and then washed three times with PBS. The supernatant was then discarded and sterilized forceps were used to remove the cover glasses. Using a drop of mounting medium with antifading (cat. no. 20210427; Beijing Solarbio Technology Co., Ltd.) the cover glasses were mounted on slides. Digital image acquisition was performed using laser confocal microscopy (Leica Microsystems GmbH).

RT-qPCR. Cells were seeded into six-well plates at a density of $1x10^6$ cells/well, allowed to attach to the bottom of the wells and then incubated with the indicated concentrations of OCT and/or LPS. Total RNA was extracted using RNAiso plus (cat. no. AM33539A; Takara Biotechnology Co., Ltd.) according to the instructions in the manual. RT was then performed using the Evo M-MLV RT Mix kit (cat. no. AG11728) and 500 ng of RNA quantified by the Nanodrop system 2000c (Thermo Fisher Scientific, Inc.) was reverse-transcribed into cDNA. The next step was real-time PCR quantification of tight ligation gene mRNA using SYBR Advantage qPCR Premix (cat. no. AG11701; Takara Bio, Inc.). A two-step program was chosen for qPCR. In step 1, the temperature was set to 95˚C for 30 sec for 1 cycle. In step 2, the temperature was set to 95˚C for 5 sec and 60˚C for 30 sec for 40 cycles. The relative mRNA expression was determined by the $2^{-\Delta\Delta Cq}$ calculation method (32). GAPDH was used as a housekeeping gene for mRNA. The target primer sequences were synthesized by Sangon Biotech. The primer sets were as follows: β-actin forward, 5'-CCTGGACTTCGAGCAAGAGATGG-3' and reverse, 5'-CAGGAAGGAAGGCTGGAAGAGTG-3'; GAPDH forward, 5'-GCACCGTCAAGGCTGAGAAC-3' and reverse, 5'-TGGTGAAGACGCCAGTGGA-3'; TNF-α forward, 5'-CCTCTCTCTAATCAGCCCTCTG-3' and reverse, 5'-GAGGACCTGGGAGTAGATGAG-3'; IL-6 forward, 5'-ACTCACCTCTTCAGAACGAATTG-3' and reverse, 5'-CCATCTTTGGAAGGTTCAGGTTG-3'; ZO-1 forward, 5'-GCGGATGGTGCTACAAGTGATG-3' and reverse, 5'-GCCTTCTGTGTCTGTGTCTTCATAG-3'; occludin (OCLN) forward, 5'-TACGGAAGTGGCTATGGCTATGG-3' and reverse, 5'-CTTTGCTGCTCTTGGGTCTGTATAG-3'; and claudin (CLDN)1 forward, 5'-TGGTGGTTGGCATCCTCCTG-3' and reverse, 5'-TCATCGTCTTCCAAGCACTTCATAC-3'.

Trans-epithelial electrical resistance (TEER). The TEER measurements across Caco-2 cell monolayers were performed using a Millicell ERS instrument (EMD Millipore). Cells were seeded with a density of $1x10^4$ per well in a 24-well Transwell plate (cat. no. 02822019; Corning, Inc.), ensuring that the liquid levels on the apicl (AP) sides and basolateral (BL) sides were at level. The fluid was changed every other day until the cells formed a tight junction on the 21st day. Before using the resistance meter, it was cleaned and set to zero with alcohol and PBS. The positive and negative electrodes were inserted into the orifice plate according to the manufacturer's instructions until the resistance meter was able to read smoothly and count. The resistance value Ω and percentage of each well were calculated according to a formula, with 3 composite wells in each group to reduce experimental errors. The TEER values of these cells after treatment were recorded. Resistance due to the cell monolayers was determined in the presence and the absence of OCT after subtracting the contribution of the blank filter. TEER was calculated as follows: TEER=(R1-R0) x A (Ω), where R1 and R0 represent the TEER readings from the wells with cells and the no-cell background wells, respectively. A (cm^2) represents the surface area of the cell monolayer on the insert.

The percentage change in TEER was calculated as follows: TEER%=TEERtest/TEERinitial x100.

Cell permeability. The cells were seeded into 24-well Transwell plates at a density of $1x10^5$ cells/well. Cells were cultured to simulate the tight junction structure of small intestinal epithelial cells. Prior to detection, Hank's balanced salt solution containing 1 mg/ml FITC-Dextran4000 (FD4; cat. no. HY-128868A; MedChemExpress) was added to the AP side of the cells and PBS was added to the BL side. FD4 (0.1 mg/ml) was added to the basal media in the Transwell chamber. Media were collected from the Transwell insert after 3 h. The fluorescence signal (excitation at 485 nm and emission at 538 nm) was measured and the FD4 concentration was calculated based on fluorescence intensity.

Transmission electron microscopy (TEM). Observation of Caco-2 cell autophagosomes was performed using a Leica TEM (Leica Microsystems GmbH). Cells were collected in 1.5-ml centrifuge tubes, fixed with glutaraldehyde (cat. no. G6257; Merck & Co., Inc.) solution overnight at 4˚C after

two washes of PBS, followed by fixation with 1% osmic acid for 1-2 h at 4˚C, three washes with PBS and gradient dehydration for 15 min per gradient. The next step was to use a gradient permeation of the embedding agent, followed by a 37˚C permeation of the pure embedding agent overnight. After heating and polymerization at 70˚C for at least 24 h, the sections were double stained with lead citrate and acetic acid peroxide oil, and then observed using a Leica TEM (Leica Microsystems GmbH).

Statistical analysis. All experiments were conducted three parallel experiments. The results in each figure are expressed as the mean ± standard error of the mean. GraphPad Prism 8 software (GraphPad; Dotmatics) was used for statistical analysis. P-values were calculated using one-way analysis of variance with Tukey's post-hoc test. $P<0.05$ was considered to indicate a statistically significant difference.

Results

OCT prevents LPS-induced intestinal epithelial cell injury in Caco2 and Sw480 cells. The effects of different concentrations of LPS on cell viability were measured in both Caco2 and Sw480 cells. The results indicated that after 24 h of incubation, 100 and 50 μg/ml LPS markedly decreased the cell viability in these two cell lines (Fig. 1A). A lower concentration of 50 μg/ml LPS was chosen for subsequent experiments. To determine whether OCT exerted any effects on the cells, they were incubated with 10, 20 and 50 μM OCT for 24 h, and cell viability was evaluated. The results suggested that OCT had no significant effect on the viability of these two cell lines (Fig. 1B). According to previous referenced results, 10 μM OCT is often used as the optimal concentration for processing cells (33). Thus, 50 μg/ml LPS and 10 μM OCT were selected for use in subsequent experiments, and Caco2 and Sw480 cells were both pre-treated with 10 μM OCT 2 h prior to treatment with 50 μg/ml LPS for 24 h. Of note, pre-treatment with 10 μM OCT significantly improved the cell viability compared with that of cells treated with LPS alone (Fig. 1C). TNF-α and IL-6 are two important pro-inflammatory cytokines that are significantly increased in IBD and the expression of these gene was measured using RT-qPCR. As indicated in Fig. 1D, LPS significantly induced the secretion of TNF-α and IL-6 in Caco2 and Sw480 cells. In addition, OCT inhibited the effects of LPS on TNF-α and IL-6 expression. Collectively, these results suggested that OCT may attenuate LPS-induced intestinal epithelial cell injury and inflammation *in vitro*.

OCT inhibits intestinal epithelial cell Caco2 damage by regulating SSTR2. To investigate which SSTR subtype has a role in the OCT-mediated protection of intestinal epithelial cells, the protein expression levels of SSTR2, -3 and -5 were examined. The results demonstrated that the expression levels of SSTR2 were significantly increased following OCT treatment, while no significant differences in SSTR3 and SSTR5 expression were observed (Fig. 2A and B). Thus, it was hypothesized that OCT may protect intestinal epithelial cells through binding to SSTR2. SSTR2 knockdown was subsequently performed using siRNA transfection (Fig. 2C). The highest level of transfection efficiency was observed following transfection with siRNA-1264 thus, siRNA-1264 was selected for use in subsequent experiments. The results demonstrated that OCT treatment did not reverse the LPS-induced reduction in Caco2 and Sw480 cell viability following SSTR2 knockdown (Fig. 2D). Furthermore, in SSTR2 knockdown cells, OCT treatment did not reverse the LPS-induced increase in pro-inflammatory cytokine expression levels (Fig. 2E).

OCT protects against LPS-induced intestinal epithelial barrier dysfunction in Caco2 cells. To further explore the effects of OCT on LPS-induced intestinal epithelial barrier dysfunction, the integrity and permeability of the intestinal epithelium were evaluated using TEER and FD4 assays in Caco2 cells. After 24 h of incubation, the resistance and permeability of cells in the control group remained at a stable level. In addition, the results revealed a significant decrease in resistance and a significant increase in FD4 permeability following LPS treatment. It was also demonstrated that cells pre-treated with OCT exhibited higher TEER values (Fig. 3A) and lower levels of FD4 permeability (Fig. 3B) as compared with cells treated with LPS alone. Following SSTR2 knockdown, OCT pre-treatment did not rescue TEER values or FD4 permeability in Caco2 cells, suggesting that OCT may preserve monolayer integrity in Caco2 cells via SSTR2.

RT-qPCR was used to investigate the expression levels of TJ proteins (Fig. 3C). The results suggested that the expression level of zo-1 was decreased after treatment with LPS; however, it was rescued after the combined treatment with LPS and OCT. No similar changes were observed in the expression of the other two tight junction molecules. Subsequently, zo-1 protein expression levels were evaluated using western blotting (Fig. 3D), and the results obtained were comparable with those observed using RT-qPCR.

OCT maintains basal levels of autophagy in Caco2 cells through SSTR2. Previous studies revealed that autophagy has an important role in maintaining the intestinal epithelial barrier by regulating TJ proteins (34,35). To determine the protective mechanisms of OCT in intestinal TJ barrier function, the formation of autophagosomes and autophagolysosomes in Caco2 cells was observed using TEM. The results indicated that intestinal epithelial cells exhibited a basal level of autophagy under normal physiological conditions; however, autophagy levels were significantly decreased following LPS treatment for 24 h. By contrast, levels of autophagy returned to baseline following treatment with OCT (Fig. 4A). Collectively, these results suggested that autophagy in Caco2 cells may have a role in the OCT-induced protection of the intestinal epithelial barrier.

As autophagy is a dynamic process, changes in the levels of autophagy were observed at different time-points. Results of the western blot analysis revealed that the ratio of LC3-II/GAPDH expression reached a maximal level after treatment for 6 h, and thereafter, the expression levels were reduced following prolonged LPS treatment. Low levels of LC3-II expression were observed in Caco2 cells following incubation for 24 h (Fig. 4B). Of note, the ratio of LC3-II/GAPDH expression also declined following OCT treatment and returned to baseline following incubation for 24 h (Fig. 4C). However, following SSTR2 knockdown, OCT treatment did not restore the levels of autophagy in Caco2 cells (Fig. 4D).

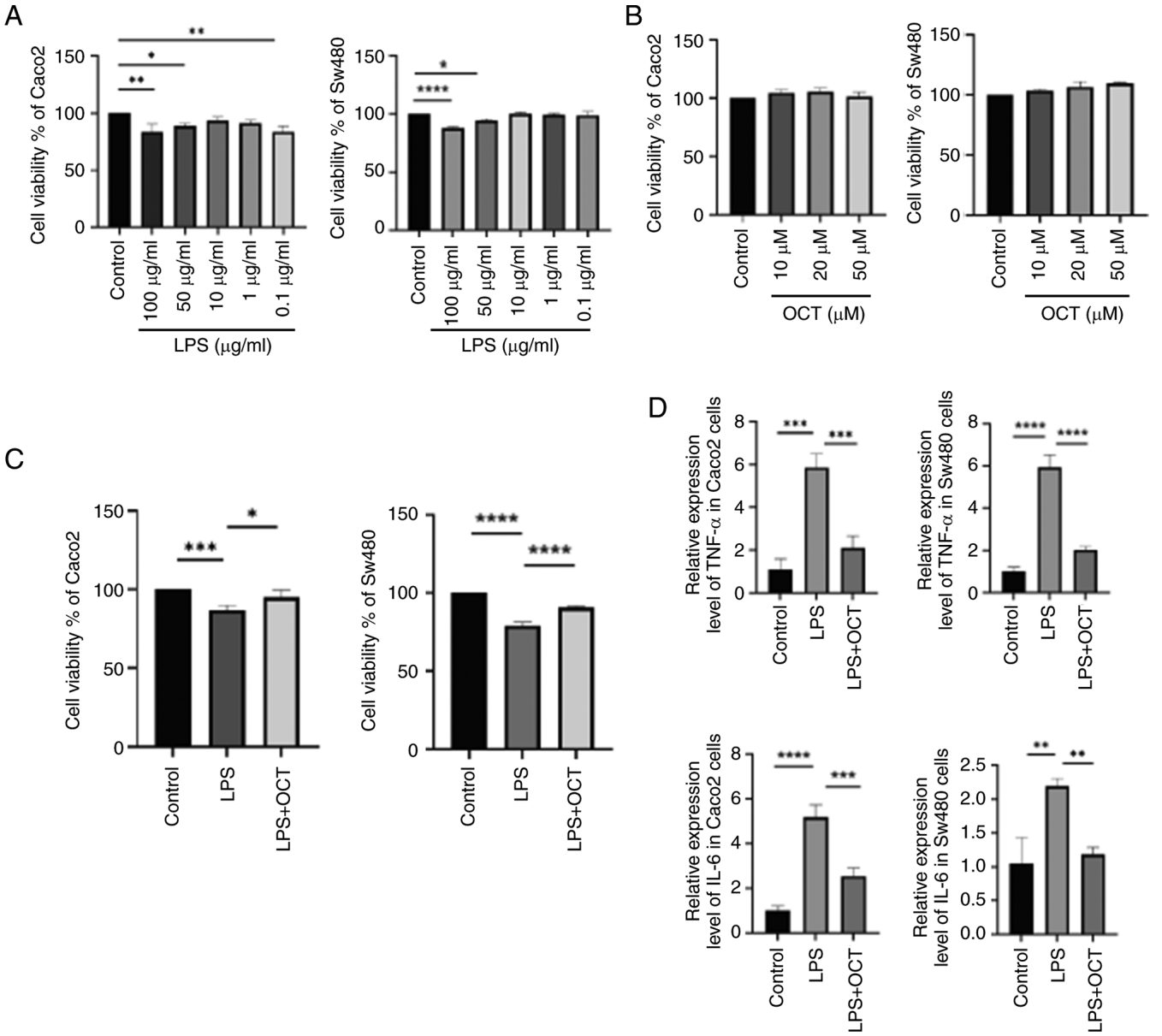

Figure 1. OCT attenuates intestinal epithelial cell injury induced by LPS in Caco2 and Sw480 cells. (A) Caco2 cells (left) and Sw480 cells (right) were incubated with LPS (0-250 μg/ml) for 24 h. (B) Caco2 cells (left) and Sw480 cells (right) were incubated with OCT (0-50 μM) for 24 h. (C) Caco2 cells (left) and Sw480 cells (right) were pretreated with OCT (10 μM) for 2 h and then stimulated with LPS (50 μg/ml) for 24 h. A CCK-8 assay was then used to detect the cell viability. (D) TGF-α and IL-6 expression in Caco2 cells and Sw480 cells were determined by reverse transcription-quantitative PCR. *P<0.05, **P<0.01, ***P<0.001, ****P<0.0001 as indicated. LPS, lipopolysaccharide; OCT, Octreotide; CKK-8, Cell Counting Kit-8.

OCT regulates changes in autophagy in Caco2 cells. Caco2 cells were transfected with the Ad-mRFP-GFP-LC3 adenovirus to assess potential changes in autophagy. In this system, the GFP signal is quenched in the acidic environment of lysosomes, whilst the mRFP signal remains stable. Therefore, autolysosomes and autophagosomes are labelled red or yellow, respectively (36). Utilizing this fluorescence peculiarity, the autophagy flux in each drug treatment group was monitored (Fig. 5A). The numbers of yellow and red dots were significantly increased following LPS treatment alone, reaching a maximal value after 6 h, before declining after 24 h (Fig. 5B). Pre-treatment with OCT also increased the numbers of yellow and red dots after 6 h, and these levels returned to baseline after 24 h (Fig. 5C). Of note, these results were comparable with those obtained in the western blot analysis of LC3-II protein expression (Fig. 4B and C).

Collectively, these results suggested that OCT may protect against LPS-induced intestinal epithelial barrier dysfunction via SSTR2. These changes may be closely associated with autophagy in intestinal epithelial cells.

Discussion

Somatostatin analogues are widely used in clinical practice (37) and are considered a safe and effective treatment option for acromegaly and acute pancreatitis (38). OCT, a somatostatin analogue, reduces damage to the intestinal mucosal barrier (39), prevents chemotherapy-induced diarrhea and other refractory diarrhea (40), and alleviates IBD and intestinal mucosal barrier injury (41). However, the mechanisms underlying the protective effects of OCT in

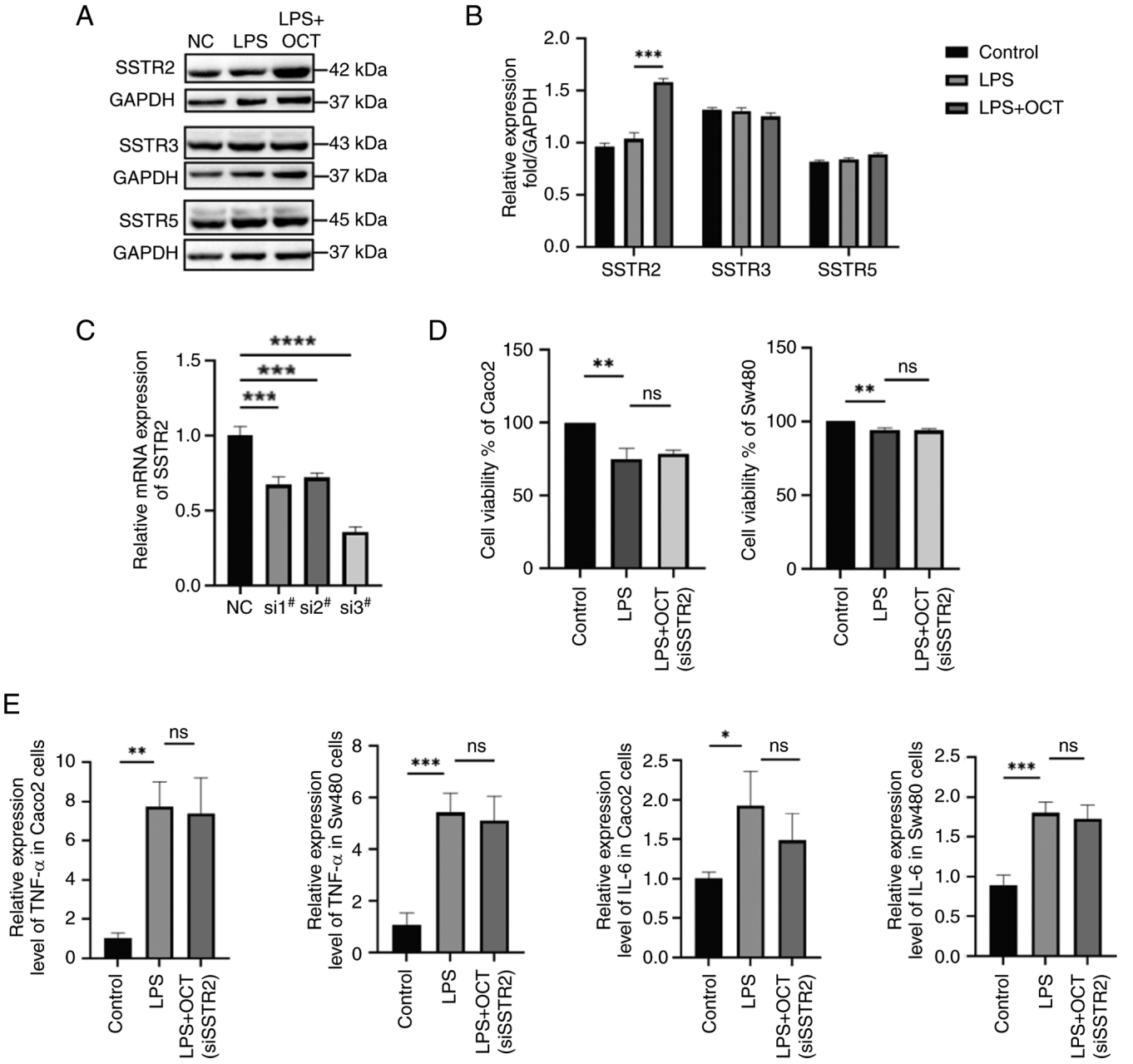

Figure 2. OCT alleviates intestinal epithelial cell damage by regulating SSTR2. (A and B) Caco2 cells were pretreated with 10 μM OCT for 2 h and then stimulated with 50 μg/ml LPS for 24 h. The protein expression levels of SSTR2, SSTR3 and SSTR5 were determined by western blot analysis. (A) Representative western blots and (B) quantified expression levels. (C) Detection of SSTR2 gene interference efficiency by RT-qPCR. (D) The Cell Counting Kit-8 assay was used to detect the viability of Caco2 cells (left) and Sw480 (right) treated with LPS (50 μg/ml) and OCT (10 μM) after interfering with SSTR2 expression. (E) TGF-α and IL-6 in Caco2 and Sw480 cells were determined by RT-qPCR. *P<0.05, **P<0.01, ***P<0.001, ****P<0.0001 as indicated; ns, no significance. RT-qPCR, reverse transcription-quantitative PCR; LPS, lipopolysaccharide; OCT, Octreotide; NC, negative control; si, small interfering RNA; SSTR, somatostatin receptor.

intestinal epithelial cells have remained elusive. Therefore, further investigations are required to determine the regulatory mechanism of OCT in intestinal epithelial cells and to explore novel targets for the treatment of diseases that cause intestinal mucosal damage.

LPS treatment of Caco2 cells is widely used to simulate intestinal mucositis *in vitro* (31,32,42). The present study aimed to determine the effects of OCT in LPS-treated Caco2 cells, using Sw480 cells for confirmation Results of the present study revealed that the LPS-induced reduction in cell viability was inhibited following OCT pre-treatment in Caco2 and Sw480 cells, suggesting that OCT may exert a protective role on the intestinal inflammatory environment. However, the role of OCT in the protection of intestinal epithelial cell injury remains unclear.

Somatostatin exerts its biological effects through interacting with SSTRs, which belong to the G-protein-coupled receptor superfamily of receptors (43,44). To date, five SSTR subtypes have been identified, namely SSTR1-5, with all five subtypes widely expressed in human tissues (14,43). Results of a previous study revealed that SSTR2 methylation may act as a prognostic indicator in colon cancer (45). SSTR1 and SSTR2 are expressed

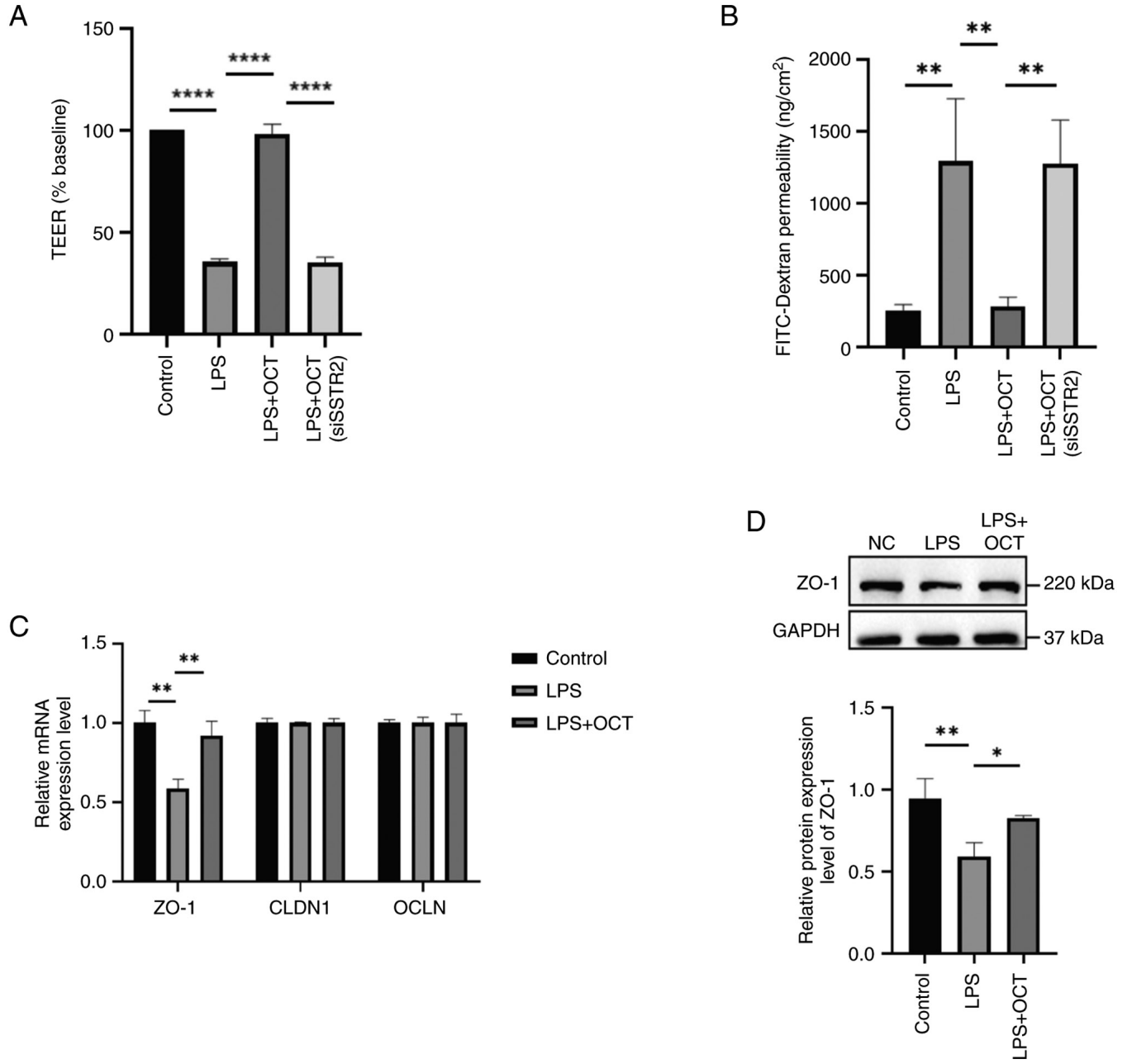

Figure 3. OCT protects against intestinal epithelial barrier dysfunction induced by LPS in Caco2 cells. (A and B) Caco2 cells were pretreated with 10 μM OCT for 2 h and then stimulated with 50 μg/ml LPS for 24 h. (A) TEER and (B) FITC-Dextran-4 flux were measured to evaluate the paracellular permeability. (C) Caco2 cells were pretreated with 10 μM OCT for 2 h and then stimulated with 50 μg/ml LPS for 24 h. The mRNA and protein expression levels of OCLN, CLDN1 and zo-1 were determined by reverse transcription-quantitative PCR and western blot analysis. (D) Caco2 cells were pretreated with 10 μM OCT for 2 h and then stimulated with 50 μg/ml LPS for 24 h. The protein expression levels of zo-1 were determined by western blot analysis. *P<0.05, **P<0.01, ****P<0.0001 as indicated. LPS, lipopolysaccharide; OCT, Octreotide; NC, negative control; si, small interfering RNA; SSTR, somatostatin receptor; CLDN, claudin; zo-1, zona occludens 1; OCLN, occludin; TEER, trans-epithelial electrical resistance.

at high levels in the colon of patients with IBD and ulcerative colitis (46,47). Of note, OCT binds to SSTR2 and SSTR5 with high affinity, and to SSTR3 with a low affinity (48). OCT does not bind to SSTR1 or SSTR4 (8). Giuliani (48) previously reported that long-acting injectable SSTR ligands, OCT and Lantenside, are suitable as first-line treatment options for patients with acromegaly (49). In addition, Valencak *et al* (23) reported that DOTA-Tyr OCT is commonly used in clinical practice for the treatment of neuroendocrine tumors, and exerts effects via binding with SSTR2 (23). In addition, results of a previous study demonstrated that OCT may be used to effectively treat patients with thymic epithelial tumors expressing SSTR2 (50). Somatostatins are used for the inhibition of inflammatory responses in clinical practice (51). Of note, the 2A subtype of SSTRs is used in the treatment of IBD, and the regulation of nerve transmission, proliferation and apoptosis (46). According to previous literature research, knockdown of SSTR is mostly concentrated in tumor model studies (52,53). For example, knockout of SSTR subtypes can improve the sensitivity of the body to induce neurological diseases (54). Downregulation of SSTR expression can promote the migration and invasion of cancer cells (55); however, knockdown models of SSTR are

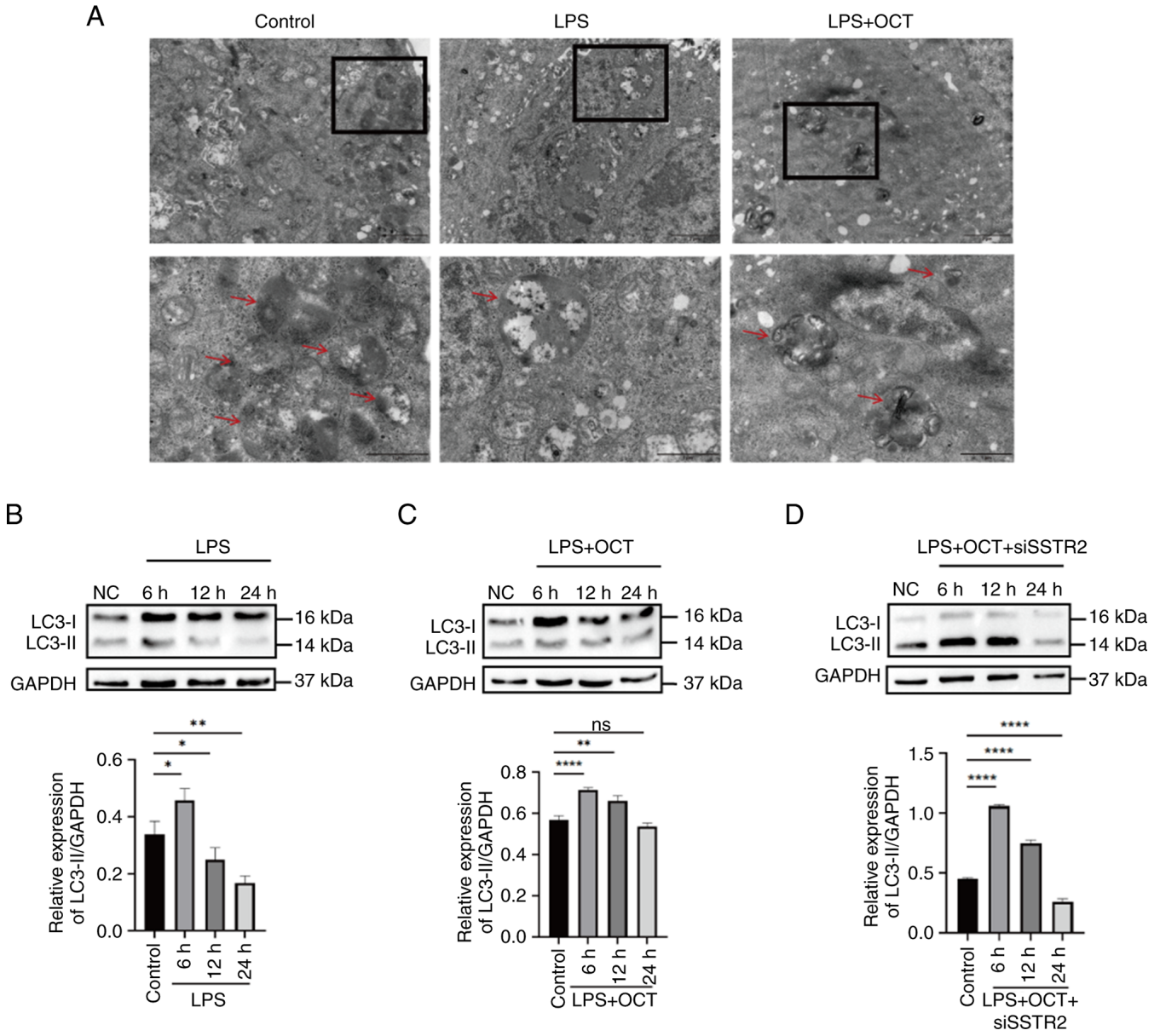

Figure 4. OCT maintains basal autophagy in Caco2 cells mediated by somatostatin receptor 2. (A) The ultrastructure of the autophagosome/autolysosome in Caco2 cells was observed with a transmission electron microscope (indicated by orange arrows; the lower panel presents the magnified windows from the upper panel. The scale bars in the upper and lower panels are 1 and 2 μM, respectively). (B) Caco2 cells were stimulated with 50 μg/ml LPS for 24 h. (C) Caco2 cells were pretreated with 10 μM OCT for 2 h and then stimulated with 50 μg/ml LPS for 24 h. (D) After interfering with SSTR2, Caco2 cells were pretreated with 10 μM OCT for 2 h and then stimulated with 50 μg/ml LPS for 24 h. The protein expression levels of LC3 protein were determined by western blot analysis at different time-points from 0 to 24 h. *P<0.05, **P<0.01, ****P<0.0001 as indicated; ns, no significance. LC, light chain; LPS, lipopolysaccharide; OCT, Octreotide; NC, negative control.

rare in inflammatory diseases. In the present cell experiments, the expression of SSTR2 was interfered with and there was no impact on other cellular functions. Thus, the potential protective effects of OCT in intestinal epithelial cells were explored in the present study. Results of the present study revealed that SSTR2 expression was significantly increased following OCT treatment in Caco2 cells. In addition, the LPS-induced reduction in cell viability was not reversed following OCT pre-treatment and SSTR2 knockdown in Caco2 and Sw480 cells, suggesting that the protective effects of OCT were inhibited following SSTR2 knockdown. Collectively, these results suggested that OCT may attenuate LPS-induced intestinal epithelial injury through regulation of SSTR2.

Damage to intestinal epithelial cells is directly associated with the function of the intestinal mucosal barrier (56). The defensive role of the intestinal epithelial barrier is dependent on intercellular TJs (57). Of note, formation of TJ protein complexes, including OCLN and zo-1, is crucial for maintaining the intestinal mucosal barrier (1). In addition, results of a previous study revealed that TJ destruction and high levels of mucosal permeability are induced by LPS (58). Results of a previous study revealed that somatostatins may mediate recovery from LPS-induced intestinal epithelial barrier dysfunction through regulation of CLDN4 (59). However, the specific molecular mechanisms or signaling pathways involved were not revealed. Results of the present study demonstrated

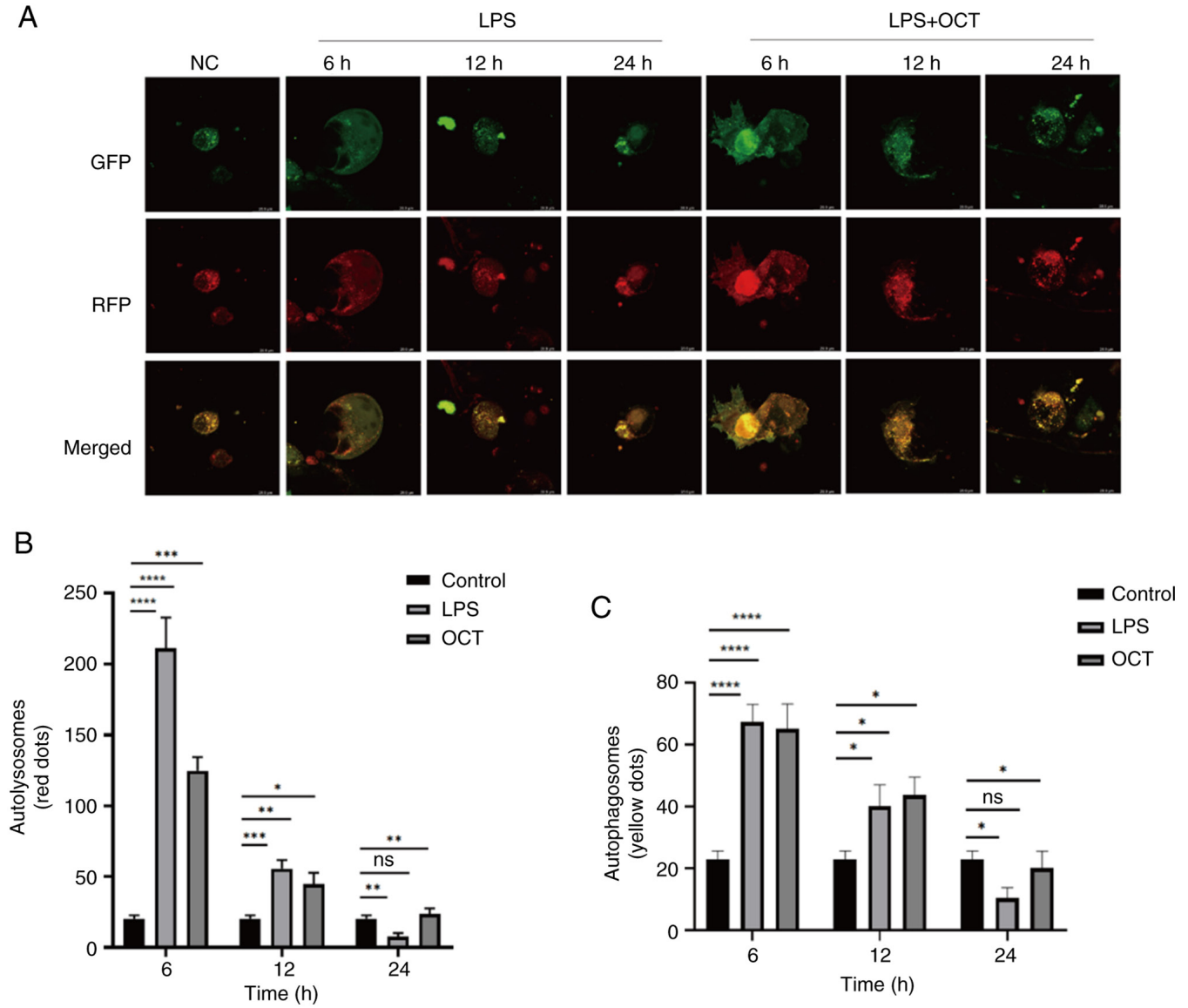

Figure 5. OCT regulates autophagy flow alteration in Caco2 cells. (A) Cells infected with autophagy double-labeled adenovirus were treated for different durations, followed by only 50 μg/ml LPS or incubation with 50 μg/ml LPS and 10 μM OCT stimulation for 24 h. Leica laser confocal microscopy was performed to detect changes in autophagy flow. The magnification of the microscope is x40. (B) The number of yellow fluorescence spots after merging of GFP and RFP (autophagosomes) in autophagic flow was counted. (C) The number of red fluorescence spots after merging of GFP and RFP (autophagolysosomes) in autophagic flow was counted. *P<0.05, **P<0.01, ***P<0.001, ****P<0.0001 as indicated; ns, no significance. LPS, lipopolysaccharide; OCT, Octreotide; NC, negative control; si, small interfering RNA; SSTR, somatostatin receptor; GFP, green fluorescence protein; RFP, red fluorescence protein.

that OCT treatment reversed intestinal barrier dysfunction in LPS-treated Caco2 cells, as evidenced by elevated TEER values, decreased FD4 flux and increased zo-1 protein expression. However, the effects of OCT were reversed following SSTR2 knockdown. These results suggested that OCT may preserve intestinal mucosal barrier function and protect intestinal epithelial cells via SSTR2.

Intestinal mucosal barrier function, particularly TJ function, is closely associated with autophagy. Results of a previous study revealed that autophagy plays an important role in maintaining intestinal epithelial barrier function through alteration of TJ protein dynamics (27). TJ dysfunction in the intestinal epithelium and defective autophagy are factors that potentiate IBD (60). Thus, research is focused on the potential interaction between autophagy and TJ proteins. Results of a previous study revealed that autophagy induced the degradation of CLDN1, which reduced the permeability of the intestinal epithelial TJ (61). Furthermore, autophagy is closely associated with CLDN proteins (62). Results of a previous study revealed that CLDN proteins are associated with increases in intestinal TJ permeability, which has a role in the intestinal pathological process (63).

Autophagy is an evolutionary mechanism that degrades cytoplasmic components, and is essential for a variety of physiological and pathological processes. Autophagy is associated with the occurrence and development of IBD (60), although the underlying mechanisms remain elusive. Results of a previous study demonstrated that defects in autophagy may exacerbate intestinal inflammation in genetically-modified mouse models (64). The results indicated the protective effects of autophagy in intestinal epithelial cells. Intestinal epithelial cells lacking autophagy

may cause epithelial barrier dysfunction. In addition, restoration of the autophagic process may ameliorate intestinal inflammation both in humans and mouse models (65). Therefore, autophagy exhibits potential as a target for regulating inflammatory response in intestinal epithelial cells. To further investigate the protective mechanisms of OCT mediated by SSTR2 in intestinal epithelial cells, autophagy was observed in the present study.

A basal level of autophagy is typically required for the maintenance of cell physiology. However, levels of autophagy are increased in response to numerous pathological processes, such as hypoxia, inflammation, infection and tumor formation, where cells attempt to survive against stress responses (66). Foerster *et al* (67) previously proposed that the crosstalk between cell stress pathways and autophagy may restore intestinal homeostasis (67). Thus, basal levels of autophagy are required for cell homeostasis.

Results of the present study revealed that the number of autophagolysosomes and autophagosomes was decreased following LPS treatment in Caco2 cells, whereas the pretreatment of OCT blunted the effects induced by LPS. Thus, autophagy may have a key role in the OCT-mediated protection of intestinal epithelial cells.

Of note, >20 autophagy-related genes (ATGs) have a role in autophagy. LC3 belongs to the ATG8 family and is a labeled protein molecule on the membrane of autophagosomes in higher eukaryotes. Following the formation of autophagosomes, LC3-I is coupled with phosphatidylethanolamine to form LC3-II, and subsequently localized in the inner and outer membranes of autophagosomes (68). LC3-II remains stable on the autophagosome membrane until it fuses with the lysosome, meaning that the level of LC3-II expression is indicative of the number of autophagosomes. Wang *et al* (69) previously reported that the extent of transformation from LC3-I to LC3-II was increased as IBD severity increased in patients, suggesting that the severity of intestinal inflammation is associated with autophagy levels (69). The most common methods used for autophagy detection are western blot analysis of LC3 conversion (LC3-II/LC3-I) and the observation of LC3 point-like aggregates using fluorescence microscopy (70). In the present study, to determine the effects of OCT on autophagy, changes in LC3 dynamics in Caco2 cells were monitored from 0 to 24 h. The results demonstrated that LC3-II protein expression levels were increased to the maximal level after treatment with LPS for 6 h, which may be indicative of a self-protective mechanism in intestinal epithelial cells when responding to pathological stress. After 12 h of LPS treatment, LC3-II protein expression levels were reduced and levels of autophagy reached the lowest point following LPS treatment for 24 h. However, levels of autophagy returned to basal levels following pre-treatment with OCT, highlighting that physiological autophagy was maintained following OCT treatment. In addition, results of the present study revealed that the regulatory effects of OCT on autophagy were inhibited following SSTR2 knockdown.

OCT is a synthetic analogue of somatostatin and exerts effects in cells by binding to SSTRs. Results of the present study revealed that basal autophagy levels in Caco2 cells are associated with OCT-mediated SSTR2 activation, leading to increased cell viability and improvements in barrier function.

In conclusion, the present study suggested that OCT-mediated SSTR2 activation may preserve intestinal mucosal barrier function by regulating autophagy in intestinal epithelial cells. Thus, OCT exhibits potential in the treatment of intestinal inflammation. In addition, the present study may provide a novel theoretical basis for the treatment of intestinal mucosal injury caused by various pathological states. However, the present study has limitations. For instance, further investigations into the molecular mechanisms underlying SSTR activation are required to identify the upstream components of the SSTR signaling pathway. In addition, the regulatory effects of OCT on the SSTR signaling pathway require further verification *in vivo*.

Acknowledgements

Not applicable.

Funding

This work was supported by the National Natural Science Foundation of China (grant no. 82000501), the Science and Technology Innovation Development Plan Project of Yantai (grant no. 2022YD068) and Xu Rongxiang Regenerative Medicine Research Program of Binzhou Medical University (grant no. BY2022XRX05).

Availability of data and materials

The data generated in the present study may be requested from the corresponding author.

Authors' contributions

XL was responsible for the implementation of *in vitro* experiments and manuscript writing. YaZ was involved in experimental data and image processing and draft revision. YuZ performed the statistical analysis and literature review. XC assisted with the study design and data analysis. DY helped with the design of experimental methods, and the literature search and collation. YL was responsible for the whole idea, project funding acquisition, experimental and manuscript framework design and manuscript revision. XL and YL confirm the authenticity of all the raw data. All authors have read and agreed to the final version of the manuscript.

Ethics approval and consent to participate

Not applicable.

Patient consent for publication

Not applicable.

Competing interests

The authors declare that they have no competing interests.

References

1. Chelakkot C, Ghim J and Ryu SH: Mechanisms regulating intestinal barrier integrity and its pathological implications. Exp Mol Med 50: 1-9, 2018.
2. Rohr MW, Narasimhulu CA, Rudeski-Rohr TA and Parthasarathy S: Negative effects of a high-fat diet on intestinal permeability: A review. Adv Nutr 11: 77-91, 2020.
3. An J, Liu Y, Wang Y, Fan R, Hu X, Zhang F, Yang J and Chen J: The role of intestinal mucosal barrier in autoimmune disease: A potential target. Front Immunol 13: 871713, 2022.
4. Shil A, Olusanya O, Ghufoor Z, Forson B, Marks J and Chichger H: Artificial sweeteners disrupt tight junctions and barrier function in the intestinal epithelium through activation of the sweet taste receptor, T1R3. Nutrients 12: 1862, 2020.
5. Chen Y, Cui W, Li X and Yang H: Interaction between commensal bacteria, immune response and the intestinal barrier in inflammatory bowel disease. Front Immunol 12: 761981, 2021.
6. Kaminsky LW, Al-Sadi R and Ma TY: IL-1β and the intestinal epithelial tight junction barrier. Front Immunol 12: 767456, 2021.
7. Zheng J, Sun Q, Zhang J and Ng SC: The role of gut microbiome in inflammatory bowel disease diagnosis and prognosis. United European Gastroenterol J 10: 1091-1102, 2022.
8. Burroughs AK and McCormick PA: Somatostatin and octreotide in gastroenterology. Aliment Pharmacol Ther 5: 331-341, 1991.
9. McKay CJ, Imrie CW and Baxter JN: Somatostatin and somatostatin analogues-are they indicated in the management of acute pancreatitis? Gut 34: 1622-1626, 1993.
10. Li X, Wang Q, Xu H, Tao L, Lu J, Cai L and Wang C: Somatostatin regulates tight junction proteins expression in colitis mice. Int J Clin Exp Pathol 7: 2153-2162, 2014.
11. Takano T, Yonemitsu Y, Saito S, Itoh H, Onohara T, Fukuda A, Takai M and Maehara Y: A somatostatin analogue, octreotide, ameliorates intestinal ischemia-reperfusion injury through the early induction of heme oxygenase-1. J Surg Res 175: 350-358, 2012.
12. Klomp MJ, Dalm SU, de Jong M, Feelders RA, Hofland J and Hofland LJ: Epigenetic regulation of somatostatin and somatostatin receptors in neuroendocrine tumors and other types of cancer. Rev Endocr Metab Disord 22: 495-510, 2021.
13. No authors listed: Somatostatin receptors: An alternative treatment target for advanced Merkel cell carcinoma. Br J Dermatol 184: e32-e52, 2021.
14. Harda K, Szabo Z, Juhasz E, Dezso B, Kiss C, Schally AV and Halmos G: Expression of somatostatin receptor subtypes (SSTR-1-SSTR-5) in pediatric hematological and oncological disorders. Molecules 25: 5775, 2020.
15. Lahlou H, Saint-Laurent N, Estève JP, Eychène A, Pradayrol L, Pyronnet S and Susini C: sst2 Somatostatin receptor inhibits cell proliferation through Ras-, Rap1-, and B-Raf-dependent ERK2 activation. J Biol Chem 278: 39356-39371, 2003.
16. Zatelli MC, Tagliati F, Taylor JE, Rossi R, Culler MD and degli Uberti EC: Somatostatin receptor subtypes 2 and 5 differentially affect proliferation in vitro of the human medullary thyroid carcinoma cell line tt. J Clin Endocrinol Metab 86: 2161-2169, 2001.
17. Colucci R, Blandizzi C, Ghisu N, Florio T and Del Tacca M: Somatostatin inhibits colon cancer cell growth through cyclooxygenase-2 downregulation. Br J Pharmacol 155: 198-209, 2008.
18. Shamsi BH, Chatoo M, Xu XK, Xu X and Chen XQ: Versatile functions of somatostatin and somatostatin receptors in the gastrointestinal system. Front Endocrinol (Lausanne) 12: 652363, 2021.
19. Fleseriu M, Dreval A, Bondar I, Vagapova G, Macut D, Pokramovich YG, Molitch ME, Leonova N, Raverot G, Grineva E, *et al*: Maintenance of response to oral octreotide compared with injectable somatostatin receptor ligands in patients with acromegaly: A phase 3, multicentre, randomised controlled trial. Lancet Diabetes Endocrinol 10: 102-111, 2022.
20. Lei S, Cheng T, Guo Y, Li C, Zhang W and Zhi F: Somatostatin ameliorates lipopolysaccharide-induced tight junction damage via the ERK-MAPK pathway in Caco2 cells. Eur J Cell Biol 93: 299-307, 2014.
21. Li Y, Li X, Geng C, Guo Y and Wang C: Somatostatin receptor 5 is critical for protecting intestinal barrier function in vivo and in vitro. Mol Cell Endocrinol 535: 111390, 2021.
22. Liew CW, Vockel M, Glassmeier G, Brandner JM, Fernandez-Ballester GJ, Schwarz JR, Schulz S, Buck F, Serrano L, Richter D and Kreienkamp HJ: Interaction of the human somatostatin receptor 3 with the multiple PDZ domain protein MUPP1 enables somatostatin to control permeability of epithelial tight junctions. FEBS Lett 583: 49-54, 2009.
23. Valencak J, Heere-Ress E, Traub-Weidinger T, Raderer M, Schneeberger A, Thalhammer T, Aust S, Hamilton G, Virgolini I and Pehamberger H: Somatostatin receptor scintigraphy with 111In-DOTA-lanreotide and 111In-DOTA-Tyr3-octreotide in patients with stage IV melanoma: In-vitro and in-vivo results. Melanoma Res 15: 523-529, 2005.
24. Glick D, Barth S and Macleod KF: Autophagy: Cellular and molecular mechanisms. J Pathol 221: 3-12, 2010.
25. Parzych KR and Klionsky DJ: An overview of autophagy: Morphology, mechanism, and regulation. Antioxid Redox Signal 20: 460-473, 2014.
26. Kim KH and Lee MS: Autophagy-a key player in cellular and body metabolism. Nat Rev Endocrinol 10: 322-337, 2014.
27. Ganapathy AS, Saha K, Suchanec E, Singh V, Verma A, Yochum G, Koltun W, Nighot M, Ma T and Nighot P: AP2M1 mediates autophagy-induced CLDN2 (claudin 2) degradation through endocytosis and interaction with LC3 and reduces intestinal epithelial tight junction permeability. Autophagy 18: 2086-2103, 2022.
28. Hu CA, Hou Y, Yi D, Qiu Y, Wu G, Kong X and Yin Y: Autophagy and tight junction proteins in the intestine and intestinal diseases. Anim Nutr 1: 123-127, 2015.
29. Rathinam VAK, Zhao Y and Shao F: Innate immunity to intracellular LPS. Nat Immunol 20: 527-533, 2019.
30. Zhang YJ and Wu Q: Sulforaphane protects intestinal epithelial cells against lipopolysaccharide-induced injury by activating the AMPK/SIRT1/PGC-1a pathway. Bioengineered 12: 4349-4360, 2021.
31. Wu XX, Huang XL, Chen RR, Li T, Ye HJ, Xie W, Huang ZM and Cao GZ: Paeoniflorin prevents intestinal barrier disruption and inhibits lipopolysaccharide (LPS)-induced inflammation in Caco-2 cell monolayers. Inflammation 42: 2215-2225, 2019.
32. Chen G, Ran X, Li B, Li Y, He D, Huang B, Fu S, Liu J and Wang W: Sodium butyrate inhibits inflammation and maintains epithelium barrier integrity in a TNBS-induced inflammatory bowel disease mice model. EBioMedicine 30: 317-325, 2018.
33. Li Y, Wang S, Gao X, Zhao Y, Li Y, Yang B, Zhang N and Ma L: Octreotide alleviates autophagy by up-regulation of MicroRNA-101 in intestinal epithelial cell line Caco-2. Cell Physiol Biochem 49: 1352-1363, 2018.
34. Saha K, Subramenium Ganapathy A, Wang A, Michael Morris N, Suchanec E, Ding W, Yochum G, Koltun W, Nighot M, Ma T and Nighot P: Autophagy reduces the degradation and promotes membrane localization of occludin to enhance the intestinal epithelial tight junction barrier against paracellular macromolecule flux. J Crohns Colitis 17: 433-449, 2023.
35. Kim Y, Lee Y, Heo G, Jeong S, Park S, Yoo JW, Jung Y and Im E: Modulation of intestinal epithelial permeability via protease-activated receptor-2-induced autophagy. Cells 11: 878, 2022.
36. Yu T, Guo F, Yu Y, Sun T, Ma D, Han J, Qian Y, Kryczek I, Sun D, Nagarsheth N, *et al*: Fusobacterium nucleatum promotes chemoresistance to colorectal cancer by modulating autophagy. Cell 170: 548-563.e16, 2017.
37. Hejna M, Schmidinger M and Raderer M: The clinical role of somatostatin analogues as antineoplastic agents: Much ado about nothing? Ann Oncol 13: 653-668, 2002.
38. Stueven AK, Kayser A, Wetz C, Amthauer H, Wree A, Tacke F, Wiedenmann B, Roderburg C and Jann H: Somatostatin analogues in the treatment of neuroendocrine tumors: Past, present and future. Int J Mol Sci 20: 3049, 2019.
39. Vockel M, Breitenbach U, Kreienkamp HJ and Brandner JM: Somatostatin regulates tight junction function and composition in human keratinocytes. Exp Dermatol 19: 888-894, 2010.
40. Sun JX and Yang N: Role of octreotide in post chemotherapy and/or radiotherapy diarrhea: Prophylaxis or therapy? Asia Pac J Clin Oncol 10: e108-e113, 2014.
41. Rao S, Viola A, Ksissa O and Fries W: Ménétrier's disease in a patient with refractory ulcerative colitis: A clinical challenge and review of the literature. BMJ Case Rep 14: e246137, 2021.
42. Wang JW, Pan YB, Cao YQ, Wang C, Jiang WD, Zhai WF and Lu JG: Loganin alleviates LPS-activated intestinal epithelial inflammation by regulating TLR4/NF-κB and JAK/STAT3 signaling pathways. Kaohsiung J Med Sci 36: 257-264, 2020.

43. Møller LN, Stidsen CE, Hartmann B and Holst JJ: Somatostatin receptors. Biochim Biophys Acta 1616: 1-84, 2003.
44. Grant M and Kumar U: The role of G-proteins in the dimerisation of human somatostatin receptor types 2 and 5. Regul Pept 159: 3-8, 2010.
45. Li J, Chen C, Bi X, Zhou C, Huang T, Ni C, Yang P, Chen S, Ye M and Duan S: DNA methylation of CMTM3, SSTR2, and MDFI genes in colorectal cancer. Gene 630: 1-7, 2017.
46. Caruso ML, Di Pinto F, Ignazzi A, Coletta S, Valentini AM, Cavalcanti E and De Michele F: Increased nerve twigs in small intestinal mucosa with programmed cell death-ligand 1 and somatostatin receptor type 2A expression in recurrent Crohn disease: A case report. Medicine (Baltimore) 97: e13492, 2018.
47. Gomes-Porras M, Cárdenas-Salas J and Álvarez-Escolá C: Somatostatin analogs in clinical practice: A review. Int J Mol Sci 21: 1682, 2020.
48. Giuliani C: The flavonoid quercetin induces AP-1 activation in FRTL-5 thyroid cells. Antioxidants (Basel) 8: 112, 2019.
49. Silverstein JM: Hyperglycemia induced by pasireotide in patients with Cushing's disease or acromegaly. Pituitary 19: 536-543, 2016.
50. Roden AC, Rakshit S, Johnson GB, Jenkins SM and Mansfield AS: Correlation of somatostatin receptor 2 expression, 68Ga-DOTATATE PET scan and octreotide treatment in thymic epithelial tumors. Front Oncol 12: 823667, 2022.
51. Periferakis A, Tsigas G, Periferakis AT, Badarau IA, Scheau AE, Tampa M, Georgescu SR, Didilescu AC, Scheau C and Caruntu C: Antitumoral and anti-inflammatory roles of somatostatin and its analogs in hepatocellular carcinoma. Anal Cell Pathol (Amst) 2021: 1840069, 2021.
52. Alexander N, Marrano P, Thorner P, Naranjo A, Van Ryn C, Martinez D, Batra V, Zhang L, Irwin MS and Baruchel S: Prevalence and clinical correlations of somatostatin receptor-2 (SSTR2) expression in neuroblastoma. J Pediatr Hematol Oncol 41: 222-227, 2019.
53. Lechner M, Schartinger VH, Steele CD, Nei WL, Ooft ML, Schreiber LM, Pipinikas CP, Chung GT, Chan YY, Wu F, *et al*: Somatostatin receptor 2 expression in nasopharyngeal cancer is induced by Epstein Barr virus infection: Impact on prognosis, imaging and therapy. Nat Commun 12: 117, 2021.
54. Gonzalez B, Vargas G, Ramirez C, Asa S, Cheng S, Sandoval C and Mercado M: Cytoplasmic expression of SSTR2 and 5 by immunohistochemistry and by RT/PCR is not associated with the pharmacological response to octreotide. Endocrinol Nutr 61: 523-530, 2014 (In English, Spanish).
55. Chen W, Ding R, Tang J, Li H, Chen C, Zhang Y, Zhang Q and Zhu X: Knocking Out SST gene of BGC823 gastric cancer cell by CRISPR/Cas9 enhances migration, invasion and expression of SEMA5A and KLF2. Cancer Manag Res 12: 1313-1321, 2020.
56. Di Tommaso N, Gasbarrini A and Ponziani FR: Intestinal barrier in human health and disease. Int J Environ Res Public Health 18: 12836, 2021.
57. Dokladny K, Zuhl MN and Moseley PL: Intestinal epithelial barrier function and tight junction proteins with heat and exercise. J Appl Physiol (1985) 120: 692-701, 2016.
58. Mohammad S and Thiemermann C: Role of metabolic endotoxemia in systemic inflammation and potential interventions. Front Immunol 11: 594150, 2020.
59. Li E, Horn N and Ajuwon KM: EPA and DHA inhibit endocytosis of claudin-4 and protect against deoxynivalenol-induced intestinal barrier dysfunction through PPARγ dependent and independent pathways in jejunal IPEC-J2 cells. Food Res Int 157: 111420, 2022.
60. Larabi A, Barnich N and Nguyen HTT: New insights into the interplay between autophagy, gut microbiota and inflammatory responses in IBD. Autophagy 16: 38-51, 2020.
61. Kim J, Choi S, Kim JO and Kim KK: Autophagy-mediated upregulation of cytoplasmic claudin 1 stimulates the degradation of SQSTM1/p62 under starvation. Biochem Biophys Res Commun 496: 159-166, 2018.
62. Yang Z, Lin P, Chen B, Zhang X, Xiao W, Wu S, Huang C, Feng D, Zhang W and Zhang J: Autophagy alleviates hypoxia-induced blood-brain barrier injury via regulation of CLDN5 (claudin 5). Autophagy 17: 3048-3067, 2021.
63. Suzuki T: Regulation of the intestinal barrier by nutrients: The role of tight junctions. Anim Sci J 91: e13357, 2020.
64. Zhou C, Li L, Li T, Sun L, Yin J, Guan H, Wang L, Zhu H, Xu P, Fan X, *et al*: SCFAs induce autophagy in intestinal epithelial cells and relieve colitis by stabilizing HIF-1α. J Mol Med (Berl) 98: 1189-1202, 2020.
65. Jia J, Gong X, Zhao Y, Yang Z, Ji K, Luan T, Zang B and Li G: Autophagy enhancing contributes to the organ protective effect of alpha-lipoic acid in septic rats. Front Immunol 10: 1491, 2019.
66. Tang C, Livingston MJ, Liu Z and Dong Z: Autophagy in kidney homeostasis and disease. Nat Rev Nephrol 16: 489-508, 2020.
67. Foerster EG, Mukherjee T, Cabral-Fernandes L, Rocha JDB, Girardin SE and Philpott DJ: How autophagy controls the intestinal epithelial barrier. Autophagy 18: 86-103, 2022.
68. Tanida I, Ueno T and Kominami E: LC3 conjugation system in mammalian autophagy. Int J Biochem Cell Biol 36: 2503-2518, 2004.
69. Wang SL, Shao BZ, Zhao SB, Chang X, Wang P, Miao CY, Li ZS and Bai Y: Intestinal autophagy links psychosocial stress with gut microbiota to promote inflammatory bowel disease. Cell Death Dis 10: 391, 2019.
70. Mizushima N and Yoshimori T: How to interpret LC3 immunoblotting. Autophagy 3: 542-545, 2007.